Analysis of Soil Liquefaction during the Recent Canterbury (New Zealand) Earthquakes

RP Orense[1], MJ Pender[2] and LM Wotherspoon[3]
[1]*Department of Civil & Environmental Engineering, University of Auckland, Auckland, New Zealand*
[2]*Department of Civil & Environmental Engineering, University of Auckland, Auckland, New Zealand*
[3]*Department of Civil & Environmental Engineering, University of Auckland, Auckland, New Zealand*
E-mail: r.orense@auckland.ac.nz, m.pender@auckland.ac.nz, l.wotherspoon@auckland.ac.nz

ABSTRACT: Four successive large-scale earthquakes, with moment magnitudes (M_w) ranging from 5.9 to 7.1, struck the Canterbury region on the South Island of New Zealand within a period of 15 months in 2010-2011. These earthquakes caused extensive damage to lifelines and residential houses in Christchurch City and adjacent areas due to widespread liquefaction and re-liquefaction in areas close to major streams, rivers and wetlands. In this paper, various analyses were made considering the results of the reconnaissance work conducted immediately after the events, the acceleration records at strong motion sites and the available boring information. The liquefaction risk in the city was evaluated to explain the severity and extent of damage during the 2010 and 2011 events. Finally, simulation of recorded ground motions through 1D effective stress ground response analysis gave a better understanding of the dynamic properties of Christchurch soils.

1. INTRODUCTION

The Canterbury region in the South Island of New Zealand experienced widespread damage due to liquefaction induced by seismic shaking during the 4 September 2010 Darfield earthquake and the large aftershocks that followed, notably those that occurred on 22 February and 13 June 2011. Ground subsidence, loss of bearing capacity and lateral spreading caused damage to houses, lifelines, and other infrastructures, particularly in Christchurch City and other outlying towns.

To understand the degree and extent of liquefaction observed, analyses were made using the recorded ground motions and the characteristics of Christchurch site and soils to evaluate the distribution of liquefaction risk in the city. In addition, attempts were made to reproduce the recorded motions at strong motion stations through effective stress analysis to better understand the ground response when subjected to different levels of shaking.

2. BACKGROUND

2.1 Geologic Setting

The Canterbury Plains comprise fans deposited by the Waimakariri and Rakaia rivers that originate from the Southern Alps. The fan covers an area approximately 50 km wide by 160 km long. Soils that make up the plains are variable, being derived from the Southern Alps greywacke and ranging from fine silts to coarse gravel and deposited in meandering river and stream beds (Brown and Weeber, 1992).

Christchurch is located on the east coast of the Canterbury Plains. The city is mainly constructed on reclaimed swamp, behind dune sand and drained estuaries (Brown and Weeber, 1992). The surface geology of Christchurch is primarily made up of Holocene alluvial gravels, sands and silts of the Springston Formation, which are highly susceptible to liquefaction, and of Christchurch Formation, which comprises denser dune and beach sands and is

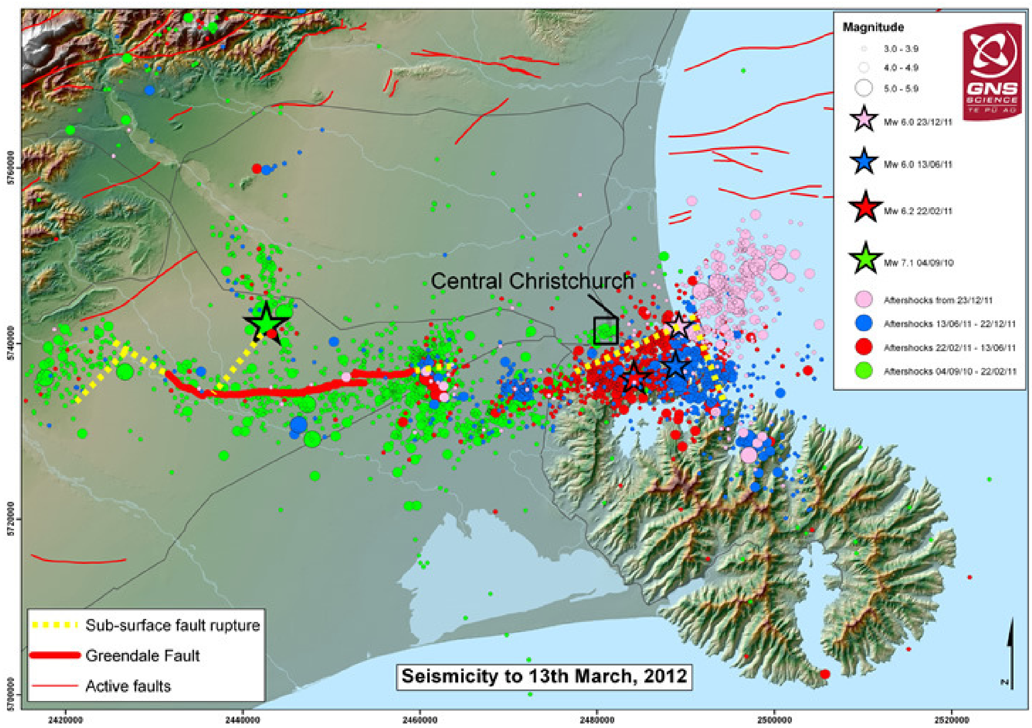

Figure 1 Earthquake epicenters, fault locations and aftershock plots following the 2010 Darfield earthquake (map courtesy of GNS Science). More than 9,000 aftershocks have been recorded since September 2010

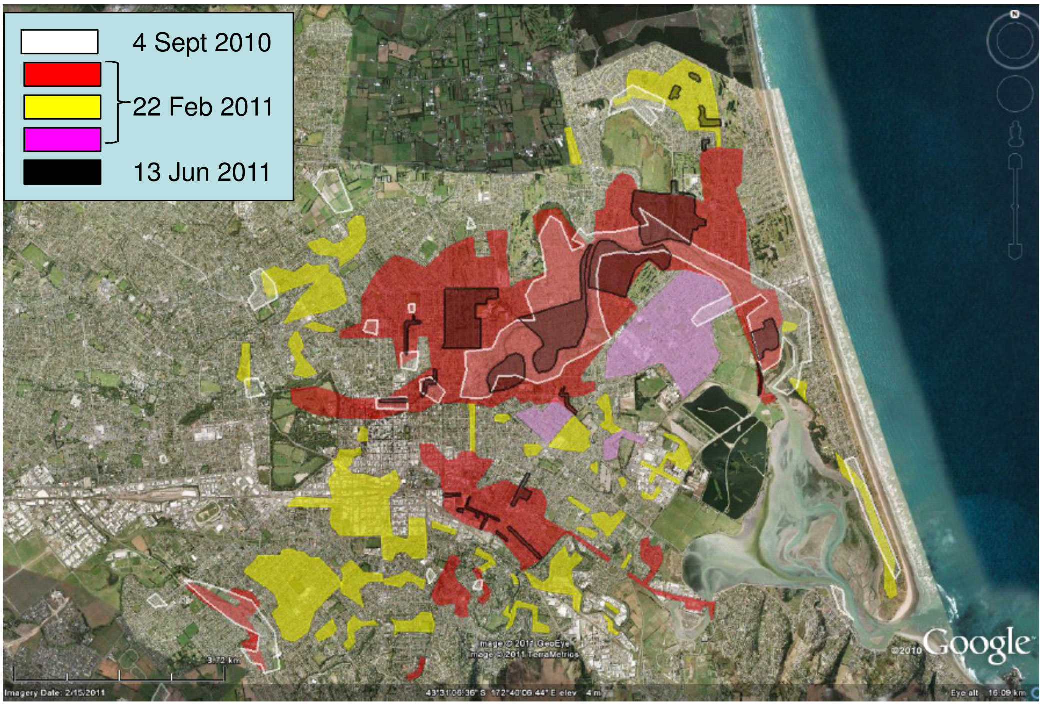

Figure 2 Observed liquefaction zones following the three events. White zone corresponds to the 4 September 2010 earthquake; red zone (severe liquefaction), yellow zone (moderate liquefaction) and pink zone (traces of liquefaction) are for the 22 February earthquake; and black zone is for 13 June 2011 earthquake. Map courtesy of M. Cubrinovski

less susceptible to liquefaction. The location of the rivers in Christchurch is of particular relevance to the liquefaction that occurred during the Darfield earthquake and its aftershocks. In Christchurch, the two main rivers, the Avon and Heathcote, originate from springs in the west and they meander through the city reworking surface sediments and creating deposits of sands and silts. The groundwater table is 2 to 3 m below the ground surface in the western suburbs and between 0 and 2 m in the central and eastern suburbs of the city.

2.2 The Earthquakes

The 4 September 2010 Darfield earthquake was of magnitude M_w=7.1 with an epicenter located 10 km southeast of the small town of Darfield, which is approximately 40 km west of Christchurch. The earthquake event, which had a focal depth of approximately 10 km, was considered complex as it involved multiple failure planes (Gledhill et al., 2011), with the majority of the earthquake-generated moment being released through the previously unmapped Greendale fault. Fortunately, there were no fatalities, in part a consequence of the time of day the earthquake occurred.

Several major aftershocks occurred following the September earthquake, the most damaging of which occurred on 22 February 2011 with a magnitude M_w=6.2. The earthquake, referred to as the Christchurch earthquake, occurred on the previously unmapped Port Hills fault located in the Port Hills south of Christchurch, at a focal depth of 5 km. The faulting was primarily reverse in mechanism, and does not appear to have caused a surface trace. The distance from the epicenter to the center of Christchurch was about 8 km, but the rupture plane was directly beneath some of the southern neighborhoods of Christchurch. Because of its shallower depth and proximity to the population center, the earthquake resulted in 181 fatalities and severely damaged thousands of residential and commercial buildings (Orense et al., 2011).

Less than four months later, the city was again rocked by a series of aftershocks on 13 June 2011, the largest of which were of magnitudes M_w=5.3 and 6.0. Although there were no casualties, there was further damage to the city's infrastructure, not to mention the additional emotional burden to the local people who experienced several thousand perceptible aftershocks since September 2010. More recent aftershocks occurred on 23 December 2011, the largest of which had a magnitude M_w=5.9.

The epicenters of the four largest earthquakes are illustrated in Figure 1. Note that the epicenter of the 2011 Christchurch Earthquake is located on an unmapped fault which is different from the Greendale Fault and it is considered as an aftershock because it was caused by a fault rupture within the zone of aftershocks that followed the September 2010 main shock (NHRP, 2011).

2.3 Liquefaction-induced damage

Although structural failure of commercial buildings led to the greatest casualties in the M_w 6.2 Christchurch earthquake, by far the most significant damage to residential buildings and lifelines in all the earthquake events was the result of liquefaction and associated ground deformations. Liquefaction occurred in areas which are known to have high potential for liquefaction – former river channels, abandoned meanders, wetlands, and ponds. Immediately following some of the largest aftershocks from the M_w 7.1 earthquake, liquefaction re-occurred in some of these areas. During the M_w 6.2 earthquake, liquefaction was more widespread and vents continued to surge during the aftershocks immediately following this event. The impact of sand boils and cracks caused by lateral spreading was that parts of the eastern suburbs were inundated with sand and silt – in places there were layers of ejected soil that were many tens of centimeters thick. The series of large aftershocks which shook the city on 13 June 2011 caused extensive re-liquefaction in many parts of the city. Streets were again flooded with water and ejected sands, reminiscent of what happened immediately after the February 2011 earthquake. Similar things were observed after the 23 December 2011 aftershock, although at smaller scale. Such re-occurrence of liquefaction indicates that the soil deposits in the area were still loose even after the intense shaking they have been subjected to over the previous 15 months.

Figure 2 illustrates the zones of liquefaction during the three events as observed from on-foot ground inspections and drive-through reconnaissance work conducted by the University of Canterbury team, with input from the University of Auckland, NZ-

GEER and Japanese Geotechnical Society (JGS) teams. The zone of liquefaction was largest following the 22 February event and several sites re-liquefied more than once.

Following the 2010 Darfield Earthquake, the New Zealand Earthquake Commission (EQC) directed a thorough investigation of the ground profile and soil characteristics in Christchurch city and adjacent areas. Figure 3 illustrates cone penetration test (CPT) results obtained at almost the same spot in Burwood, north of the Avon River. It is observed that the site consists of 6-7 m thick of loose sandy layer underlain by thick dense deposits. Note that one set of CPT soundings was taken in December 2010 after the Darfield event, while the other was taken after the 2011 Christchurch earthquake. Except for the lower ground surface, the two results are practically similar, indicating that following the liquefaction of the loose sandy deposit during the Christchurch earthquake, the ground in this area returned to its pre-earthquake strength. Kiyota et al. (2011) performed Swedish weight sounding tests in other parts of the city, such as Avonside and Bexley, on 15 September 2010 and 18 June 2011 (after the 2010 Darfield earthquake and 13 June 2011 aftershocks, respectively) and noted practically no change in the penetration resistance of the ground. Thus, it can be surmised that liquefaction and re-liquefaction of the sites did not result in densification of the loose deposit. Unless the sites are improved, future earthquakes of sufficient magnitude can again induce liquefaction.

3. ANALYSIS OF STRONG MOTION RECORDS

During the 2010 Darfield earthquake, a series of strong motion accelerographs was triggered and motions recorded at several stations installed in the Canterbury Plains. Based on GeoNet strong motion FTP site, the recorded peak ground accelerations (PGA) in Christchurch were in the order of 0.15g–0.30g, as shown in Table 1. Because the M_w=6.2 February aftershock was much closer to the Christchurch CBD than the M_w=7.1 September main shock, the ground accelerations experienced in the CBD as a result of the 2011 earthquake were 3–4 times greater than during 2010 event (see Table 1); in the eastern suburbs, they were about 5 times greater. The vertical PGA recorded was 1.47g at Heathcote Valley Primary School (about midway between the CBD and the epicenter) whilst in the CBD the PGA was 0.5g–0.7g and in the eastern suburbs the maximum recorded vertical PGA was 1.63g (GeoNet, 2011). Following the major aftershocks on 13 June 2011 (M_w=5.3 at 1:01 pm and M_w=6.0 at 2:20 pm), large vertical accelerations in the range of 0.5g–0.7g were again recorded.

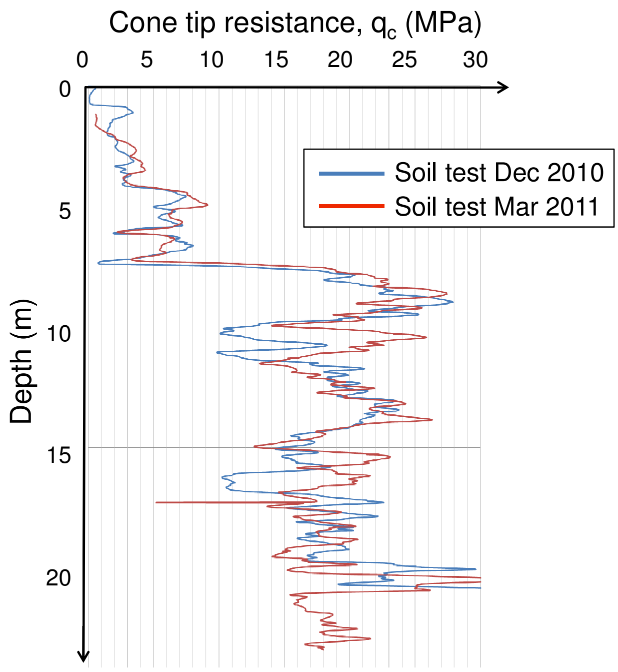

Figure 3 Cone penetration test results in Burwood taken in December 2010 and March 2011. Note the practically similar strength profiles, indicating that the ground returned to its pre-earthquake strength. Data courtesy of Tonkin & Taylor.

In order to make a meaningful comparison of the effect of ground shaking on the degree of liquefaction taking into account the different earthquake magnitudes, strong motion records from the four earthquakes monitored at four strong motion stations were compared, as shown in Table 1. Here, the cyclic shear stress ratio (*CSR*) is computed for each station and expressed in terms of the reference magnitude M_w=7.5. The *CSR* is calculated using the equation below (Seed and Idriss, 1970):

$$CSR = 0.65 \frac{a_{\max}}{g} \frac{\sigma_v}{\sigma_v'} r_d \tag{1}$$

where $a_{\max}$ is the peak horizontal acceleration at the ground surface, σ_v and σ_v' are the total and effective stresses at the depth under consideration, g is the acceleration due to gravity, and r_d is a stress reduction coefficient to account for the flexibility of the soil profile.

Table 1 Comparison of strong motion records during the four devastating earthquakes.

Seismic stations	2010 Darfield Earthquake (M_w=7.1; *MSF*=1.15)			2011 Christchurch Earthquake (M_w=6.2; *MSF*=1.63)			13 June 2011 Earthquake – 1:01pm (M_w=5.3; *MSF*=2.43)			13 June 2011 Earthquake – 2:20pm (M_w=6.0; *MSF*=1.77)		
	Vert	Max Hor	$CSR\|_{7.5}$	Vert	Max Hor	$CSR\|_{7.5}$	Vert	Max Hor	$CSR\|_{7.5}$	Vert	Max Hor	$CSR\|_{7.5}$
PRPC	0.31	0.23	0.13	1.63	0.73	0.29	0.65	0.34	0.09	0.69	0.48	0.18
REHS	0.21	0.33	0.19	0.53	0.73	0.29	0.22	0.27	0.07	0.17	0.35	0.13
HPSC	0.13	0.16	0.09	0.86	0.25	0.10	0.51	0.20	0.05	0.36	0.42	0.15
SHLC	0.12	0.19	0.11	0.50	0.34	0.14	0.12	0.30	0.08	0.14	0.22	0.08
Observed Liquefaction	Low to moderate			Severe			Low to moderate					

Note: PRPC: Pages Road Pumping Station; REHS: Christchurch Resthaven; HPSC: Hulverstone Drive Pumping Station; SHLC: Shirley Library; Vert – vertical acceleration; Max. Hor – calculated maximum resultant acceleration of horizontal components; $CSR|_{7.5}$: cyclic stress ratio at M_w=7.5. Unit of acceleration is g (1 g = 980 cm/s^2). Source of acceleration data: GeoNet 2011.

To simplify the analysis, the *CSR* at the location of the water table, assumed at GL-1.0m, was evaluated. For earthquake magnitudes other than 7.5, the factor of safety was adjusted by a magnitude scaling factor, *MSF* (Youd et al. 2001):

$$MSF = \frac{10^{2.24}}{M_w^{\ 2.56}} \tag{2}$$

The cyclic stress ratio *CSR* indicated in the table is taken as $CSR|_{7.5}=CSR/MSF$. In this way, the effects of both amplitude of acceleration and the number of significant cycles (or duration) can be incorporated into a single parameter.

From the table, it can be deduced that severe liquefaction occurred when the values of $CSR|_{7.5}$ were in the range of 0.25 – 0.30, while between 0.15 – 0.20, low to moderate liquefaction was observed. On the other hand, no liquefaction was observed when $CSR|_{7.5}$ is < 0.10. Indeed, severe liquefaction was observed during the February 2011 earthquake, while low to moderate degree of liquefaction was noted in the September 2010 and June 2011 events. This is reflected in the liquefaction maps shown in Figure 2. Note that since the two major aftershocks that occurred on 13 June 2011 were only 80 minutes apart, the liquefaction effects produced by the second earthquake were amplified because there were still elevated excess pore water pressures in the ground induced by the first earthquake.

4. EVALUATION OF LIQUEFACTION RISK

The threat of liquefaction in the Canterbury Region has been known for some time. For example, studies, such as those performed by Beca (2002), have assessed the liquefaction hazard in Christchurch. Whilst these studies have produced liquefaction hazard maps, they have failed to quantify the damage expected due to liquefaction. In this section, simplified procedures were used to calculate the distribution of liquefaction potential index (LPI), which was proposed by Iwasaki et al. (1984), at various sites in Christchurch for both the September 2010 and February 2011 earthquake events. A comparison is then made between the calculated LPI distribution and the actual liquefaction damage mapped to explain the ground characteristics and to quantify the risk in the city.

4.1 Input parameters

As mentioned earlier, EQC commissioned a detailed investigation of Christchurch following the September 2010 earthquake, including many cone penetration tests (CPT), and the data were compiled by Tonkin & Taylor (2010). In this study, a representative CPT result was taken for each 200 m x 200 m mesh adopted for the affected suburbs. Where possible, CPTs near adjacent boreholes were selected for better insight on actual ground conditions; overall, 115 CPTs were analysed. It was tacitly assumed that the soil strength profiles were essentially the same following the 2010 and 2011 earthquakes, as illustrated by a typical profile shown in Figure 3.

For the September 2010 event, the groundwater was estimated from the CPT results and where possible checked against the groundwater well logs of Environment Canterbury (ECan). For the February 2011 event, groundwater well logs from ECan were analysed to determine the average change in groundwater levels in the region. It is worth mentioning that the groundwater levels in February 2011 were found to be higher by about 800 mm in Christchurch when compared to September 2010, possibly due to the snow melting in the Southern Alps which recharged the Canterbury Plains.

Distributions of peak horizontal ground accelerations (PHAs) were determined from the GeoNet recordings and the geometric mean of the two horizontal directions were used in the analysis of both the 2010 and 2011 earthquakes.

4.2 Factor of Safety against Liquefaction

To evaluate the factor of safety against liquefaction, the seismic demand on a soil layer (or the cyclic stress ratio, *CSR*) and the capacity of the soil to resist liquefaction (or the cyclic resistance ratio, *CRR*) need to be determined (Youd et al., 2001). The *CSR* was calculated using Equation (1) while the *CRR* was estimated using CPT results. Robertson and Wride (1998) developed a technique to estimate the *CRR* by first evaluating the soil type from the CPT considering that the CPT friction ratio generally increases as fines content and soil plasticity increase. The soil behaviour index, I_c, can be calculated using the equations below.

$$I_c = \left[(3.47 - \log Q_{tn})^2 + (1.22 + \log F)^2\right]^n \tag{3}$$

where

$$Q_{tn} = \left(\frac{q_c - \sigma_v}{P_a}\right)\left(\frac{P_a}{\sigma_v'}\right)^n \tag{4a}$$

$$F = \left(\frac{f_s}{q_c - \sigma_v}\right)\times 100\% \tag{4b}$$

In the above equations, q_c and f_s are the tip resistance and sleeve friction, respectively, P_a is the atmospheric pressure and n is a stress component which is taken as 1.0 for clay, 0.5 for sand and between 0.5 and 1.0 for silts and sandy silts. Robertson and Cabal (2010) recommended the following procedure for calculating I_c. Clayey soils are first differentiated from sands and silts by calculating I_c assuming n = 1.0. The assumption for n is then checked using Equation (5). Iterations are then performed by recalculating I_c with updated n values until $\Delta n \le 0.01$.

$$n = 0.381 I_c + 0.05\left(\frac{\sigma_v'}{P_a}\right) - 0.15, \quad n \le 1 \tag{5}$$

For soils with I_c>2.6, the soil is classified as clayey which is considered to be non-liquefiable but should be checked for cyclic softening for low-risk projects. For high risk projects, soil samples should be retrieved and tested to complete the analysis. If I_c < 2.6, the soil is likely to be granular and the I_c is then used to estimate the liquefaction resistance (Youd et al., 2001).

For silty sands, the penetration resistance, Q_{tn}, normalised with respect to an effective overburden pressure of P_a=100 kPa is corrected to an equivalent clean sand value by the relationship:

$$(Q_{tn})_{cs} = K_c (Q_{tn}) \tag{6}$$

where K_c is a correction factor that is a function of grain characteristics (combined influence of fines content and plasticity) of the soil. It is calculated using the following equation:

$$K_c = \begin{cases} 1.0 & I_c \le 1.64 \\ 5.581 I_c^{\ 3} - 0.403 I_c^{\ 4} - 21.63 I_c^{\ 2} + 33.75 I_c - 17.88 & I_c > 1.64 \end{cases} \tag{7}$$

Once the equivalent clean sand value is known, the *CRR*, defined for M_w=7.5 earthquake, can be calculated using the following equation:

$$CRR = \begin{cases} 0.833\left[\dfrac{(Q_{tn})_{cs}}{1000}\right] + 0.05 & (Q_{tn})_{cs} < 50 \\ 93\left[\dfrac{(Q_{tn})_{cs}}{1000}\right]^3 + 0.08 & 50 \le (Q_{tn})_{cs} < 160 \end{cases} \tag{8}$$

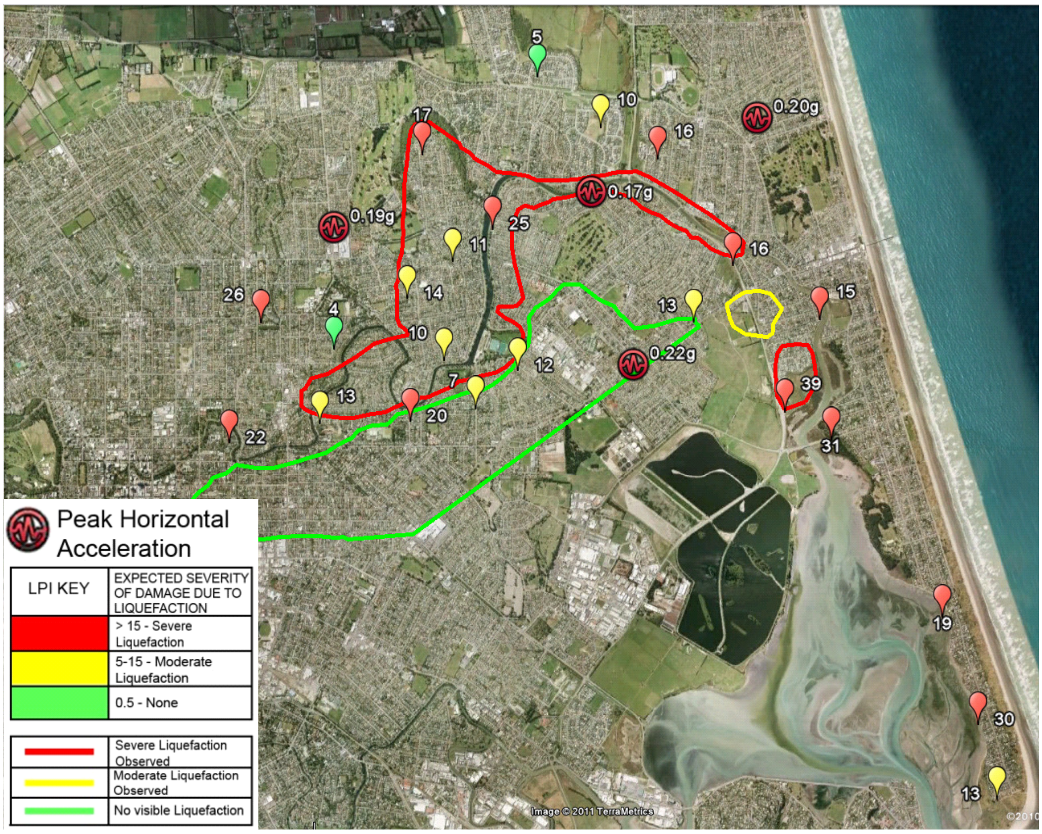

(a) September 2010 Earthquake

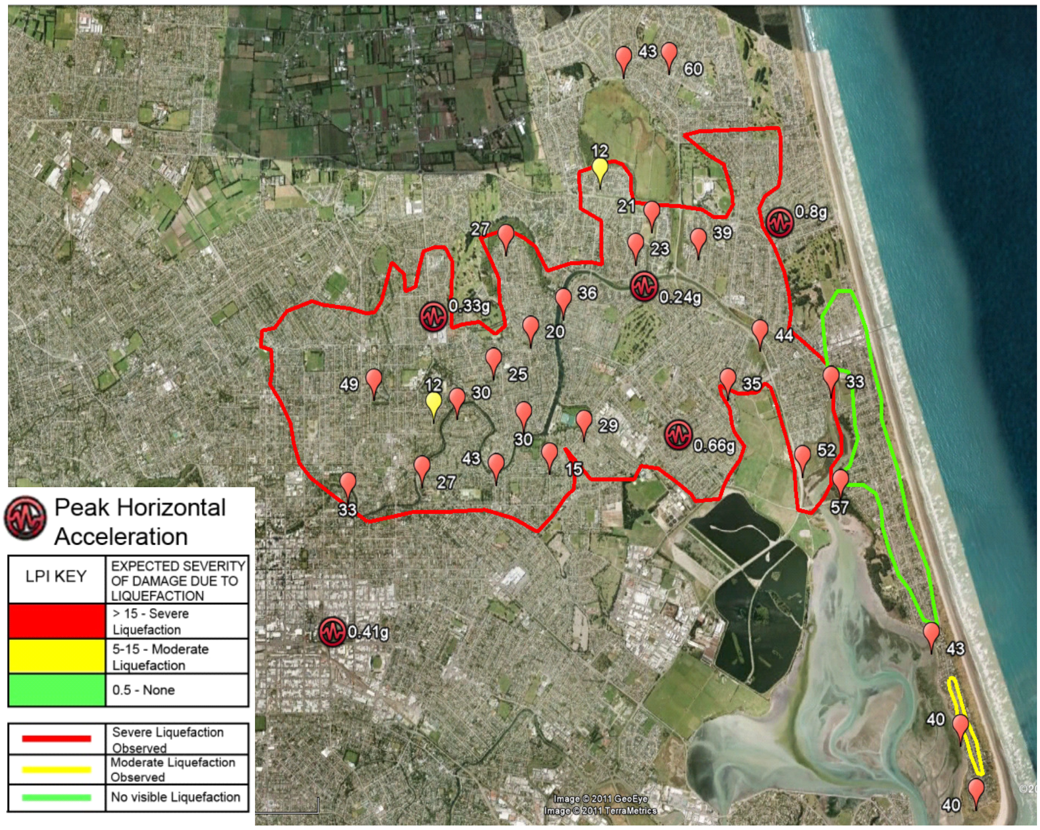

(b) February 2011 Earthquake

Figure 4 Distribution of LPIs in Christchurch for the September 2010 earthquake and February 2011 earthquake. Red dots are for LPI>15, yellow dots are for 5<LPI<15, and green dots are for LPI<5. Also plotted are the liquefaction zones based on (a) Japanese Geotechnical Society reconnaissance work (Orense et al., 2011) and (b) University of Canterbury reconnaissance work (after Cubrinovski & Taylor 2011), with the red region corresponding to severe liquefaction zone, yellow region to the moderate liquefaction zone and green region to the no visible liquefaction zone.

For earthquake magnitudes other than 7.5, the factor of safety is adjusted by a magnitude scaling factor, *MSF*, i.e.

$$F_S = \frac{CRR}{CSR} \times MSF \tag{9}$$

$F_S < 1.0$ indicates that the layer liquefies whilst $F_S > 1.0$ indicates the layer does not to liquefy under the imposed cyclic load.

4.3 Liquefaction Potential Index

Whilst the factor of safety gives an indication about whether a soil layer liquefies or not, it does not give an indication about the damage expected at the ground surface due to liquefaction. The LPI is a single number that quantifies the damage expected at the ground surface due to liquefaction. The LPI is calculated by:

$$LPI = \int_0^{20} F \times W(z)dz \tag{10}$$

where

$$F = \begin{cases} 1 - F_S & \text{for } F_S \le 1.0 \\ 0 & \text{for } F_S > 1.0 \end{cases} \tag{11a}$$

$$W(z) = 10 - 0.5z \ \text{(in m)} \tag{11b}$$

In the above equations, z is the depth from the ground surface. The weighting function $W(z)$ is triangular in shape, with maximum value (or weight) given to the top layers, where the effect of liquefaction on the ground surface is largest, and decreases with depth. The LPI is calculated up to a maximum depth of 20 m as surface effects from liquefaction for depths greater than 20 m have rarely been reported (Iwasaki et al., 1984). Based on this definition, LPI values can range from 0 for a site where the factor of safety is greater than one for the entire 20m range (no liquefaction) to a maximum of 100 for a site where the factor of safety is zero over the entire 20m range.

The methodology outlined above was implemented for Christchurch City considering the September 2010 earthquake. The distribution of LPI is shown in Figure 4(a) together with regions of observed liquefaction. The plot suggests that there is a spread in severity, with LPI < 5 on the northern side of the Avon River and in Parklands, indicating no visible liquefaction damage. LPI values in the range of 5 to 15 were found along the Avon River in Wainoni, Dallington and Burwood, as well as in New Brighton, Aranui and the southern tip of South Shore, indicating moderate liquefaction. Severe liquefaction is scattered throughout the areas of interest, with particular density in Bexley. Also indicated in the figure are the zones of liquefaction as reported by the Japanese Geotechnical Society (Orense et al. 2011). There was severe liquefaction damage mapped along the Avon River, Burwood, Dallington and parts of Bexley. No visible liquefaction damage was found on the southern side of the Avon River such as Linwood but there were localised cases of severe and moderate damage in Bexley and Aranui in the east. Based on the figure, there appears to be good correlation between the calculated LPIs and the observed severity of liquefaction.

The same approach was applied considering the February 2011 earthquake and the distribution is shown in Figure 4(b). Compared to the 2010 event, there were large changes in LPI values, with the majority of the values being >15, indicating severe liquefaction. It must be noted that a large proportion of the LPI values are actually >30, indicating a high degree of severity in damage observed during the more recent event. Among the CPTs considered, only two exhibited moderate liquefaction damage. The mapped liquefaction damage following the 2011 earthquake was carried out by the University of Canterbury (Cubrinovski & Taylor 2011). It highlights extensive and severe liquefaction damage throughout the eastern area of Christchurch; New Brighton was mapped as no visible liquefaction damage, while South Shore experienced moderate liquefaction damage.

Next, a more detailed analysis is made on the LPIs calculated and the actual damage observed. The high LPI values (LPI>15) plotted in the red areas (severe mapped liquefaction damage) indicate that the empirical method used to determine LPI was consistent with the liquefaction damage mapped. This suggests that those areas contain soil materials that are very susceptible to liquefaction, and that liquefaction was triggered during the earthquake event. This is also confirmed by the plots of low LPI values (LPI<5) in the green areas (no mapped liquefaction damage). In this category, soil materials are less likely to experience liquefaction, and liquefaction was not triggered during the earthquake event.

Note, however, that there are low LPIs plotted in severe liquefaction zones, as well as high LPIs on no liquefaction zones. The former can be explained by the occurrence of lateral spreading, i.e., the empirical methods of determining the LPI are based upon level ground liquefaction (Youd et al., 2001), whereas mapped observations consider other deformation modes. Consequently, areas which may not have experienced severe level ground liquefaction may have been in an area that experienced lateral spreading (Robinson et al. 2011) and therefore was mapped as severe liquefaction damage. The latter, on the other hand, can be traced to the effect of the thickness of surface unliquefied crust. The thick non-liquefied crust prevented surface manifestation of liquefaction, and consequently prevented liquefaction from being observed and hence mapped. A further study of this is presented in the next section.

There was a significant increase in the severity of liquefaction when comparing the February 2011 and September 2010 earthquakes. Not only were the majority of LPIs greater than 15, many were in excess of 30. This was due to the large increase in PHA, as mention in Section 2, with some PHAs increasing by as much as four times the values that were recorded during the September event. This increase, coupled with the rise in water table, created the large increase in LPI values, as summarised in Figure 5.

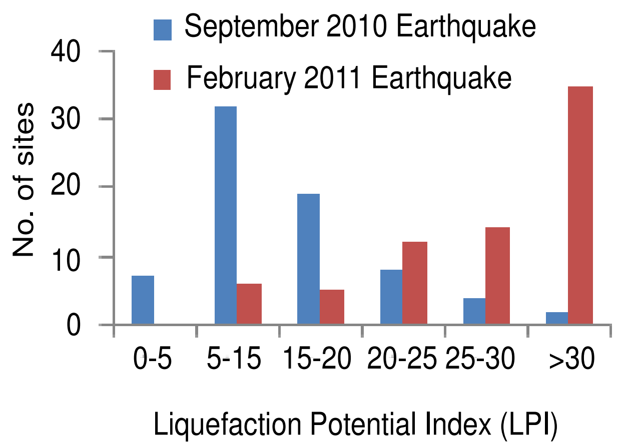

Figure 5 Comparison of Liquefaction Potential Index (LPI) between September 2010 and February 2011 earthquakes. Note the increase in number of sites with higher LPIs in the 2011 earthquake as compared to the 2010 earthquake.

4.4 Effect of Surface Crust

As mentioned above, the thickness of the non-liquefied surface crust can prevent surface manifestation of subsoil liquefaction, and consequently can prevent its manifestation on the ground surface. The relationship between the thickness of surface crust and of liquefiable deposit has been investigated by Ishihara (1985) using actual case histories where liquefaction-induced damage has or has

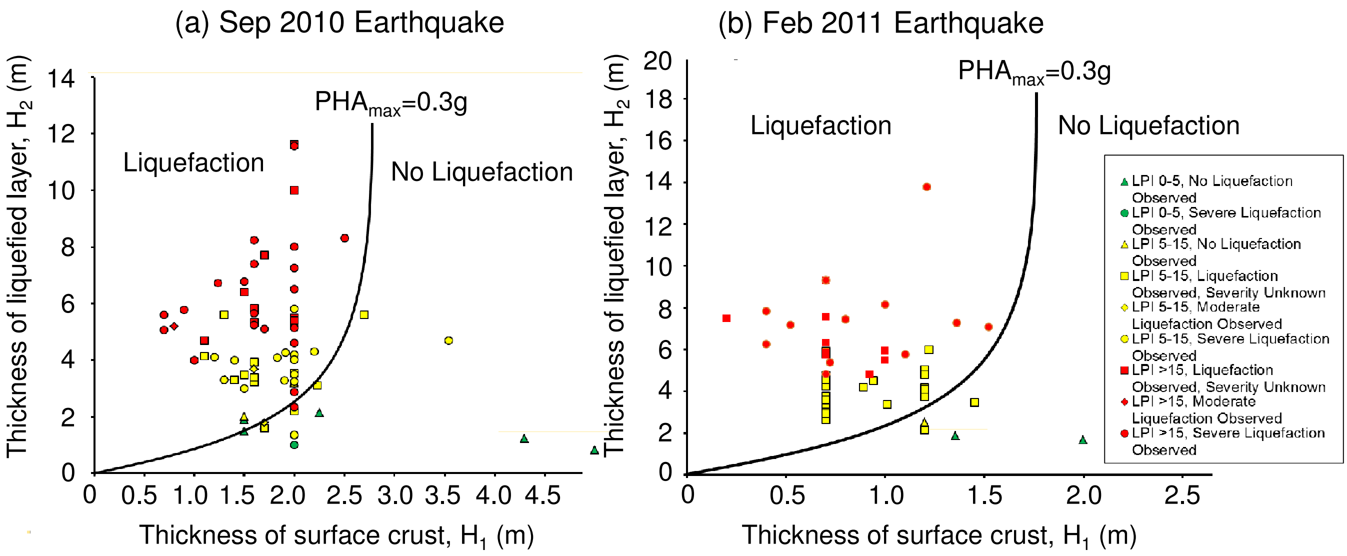

Figure 6 Relationship between the thickness of surface crust and of liquefiable layer separating manifestation of liquefaction on the surface: (a) September 2010 earthquake; and (b) February 2011 earthquake.

not been observed. Depending on the relation between the thickness of the liquefiable layer, H_2, and the thickness of surface crust, H_1, a boundary was drawn to estimate whether or not liquefaction will exert damage on the ground surface for a given peak ground acceleration (PGA).

The same methodology was adopted here considering the results of Factor of Safety calculations. The thickness of the non-liquefiable surface crust depth (H_1) and the summation of the liquefiable layers up to a maximum depth of 20 m (H_2) were plotted, and curves delineating occurrence or non-occurrence of liquefaction-induced damage from actual reconnaissance work were drawn. Boundary curves were determined for PGA=0.3 and 0.5g for the September 2010 event, while PGA=0.3g, 0.5g and 0.7g were determined for the February 2011 event. The data points were colour-coded depending on the calculated LPI values.

Figures 6(a) and 6(b) illustrate the plots for the September 2010 event and February 2011 earthquake, respectively, for PGA=0.3g. Both plots showed that sites which produced LPI values >5 but were plotted on the non-liquefied side of the boundary curve were found to have high H_1 values. As indicated above, the thick non-liquefied surface crust prevented surface manifestation of liquefaction, and consequently prevented liquefaction being observed and hence mapped.

4.5 Limitations

It is worth mentioning that although efforts were made to ensure that as many CPT sites as possible extend up to 20 m deep for analysis purposes, there were cases where the available CPT data did not. In these cases, it was assumed that layers deeper than the available depth and up to 20m had a factor of safety > 1 and did not liquefy. This potentially underestimated the LPI result. Moreover, the lack of CPT data information in some areas such as in Aranui and Eastern areas of Christchurch limits the scope of the present analyses. Most CPTs were performed in areas which liquefied after the September 2010 event, and very few information was available at sites which did not liquefy. As observed in Figure 2, the extent of liquefaction was much wider during the February 2011 earthquake, and sites which may not have liquefied during the September 2010 event, liquefied this time. As a result, no comparison could be made and hence no explanation is provided on why certain sites did not liquefy during the first event, but did in the second. Because of this, the liquefaction boundary curves shown in Figure 6 may have been underestimated.

5. EFFECTIVE STRESS ANALYSIS

In order to get a better understanding of the dynamic behaviour of Christchurch soils, an attempt was made to simulate some of the recorded motions during the September 2010 and February 2011 earthquakes by performing 1D effective stress ground response analysis. For this purpose, strain-controlled cyclic triaxial tests were performed on reconstituted soil samples obtained from Christchurch to determine the input parameters for the ground response analyses. Strong motion records at non-liquefied sites were used to calculate the engineering bedrock motion by deconvolution process after which attenuation relationships were used to estimate the amplitude of bedrock motion at the target strong motion station. Note that due to the absence of actual boring data at strong motion sites, borehole data nearest to the target sites were used. The boring information and input data were then employed in effective stress analysis to reproduce the motion at the ground surface.

5.1 Dynamic properties of Christchurch Soils

The soil sample obtained in Christchurch was sandy in nature, with the following index properties: mean diameter D_{50}=0.15mm, uniformity coefficient, C_u=1.125, fines content, F_c=3%, specific gravity of solid particles, G_s=2.66, and maximum and minimum void ratios of e_{max}=0.887 and e_{min}=0.587, respectively.

The water sedimentation method was used to form the triaxial soil specimens. Wet sand, which was previously boiled under a vacuum to remove entrapped air, was placed carefully into a mould measuring 75 mm in diameter and 150 mm high containing de-aired water. A target initial relative density D_r=48% was considered as this represents typical values in-situ based on review of CPT test results. B-value >0.95 indicated the specimen thus formed was fully saturated.

The specimen was consolidated at an effective confining pressure, σ_o'=100 kPa after which it was subjected to strain-controlled cyclic loading at 0.1Hz frequency. Three double amplitude shear strain levels were considered: γ_c=0.08%, 0.16% and 0.25%. In the triaxial tests, the applied double amplitude cyclic axial strains were calculated assuming fully undrained condition with Poisson's ratio, ν=0.5. During the tests, the excess pore water pressure, u, generated in the specimen and the cyclic deviator stress σ_d, were monitored. All tests were terminated when initial liquefaction was observed in the specimen.

A typical result of the strain-controlled triaxial tests is shown in Figure 7 corresponding to a specimen subjected to a double

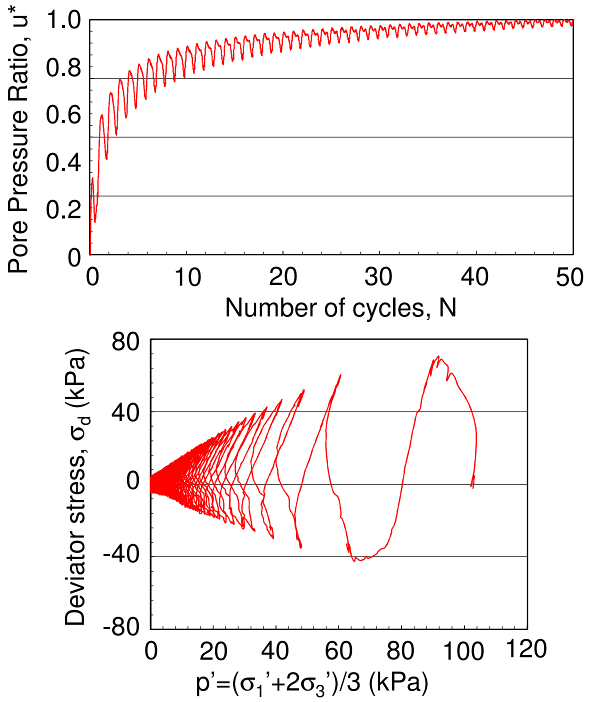

Figure 7 Results of strain-controlled cyclic triaxial test for double amplitude shear strain γ_c=0.25%. (a) Excess pore water pressure response; and (b) effective stress path.

amplitude shear strain level of γ_c=0.25%. It is observed that there was sudden development of excess pore water pressure during the initial stages of loading, but the rate of pore pressure generation decreases as the cycling straining continued. Initial liquefaction finally occurred after 46 cycles.

The results for all the tests are summarised in terms of the relationship between the inverse of the excess pore water pressure ratio ($u^*=u/\sigma_o'$) and the inverse of the number of loading cycles, N, and this is shown in Figure 8 for the three different cyclic strain amplitude levels. It is observed that the relationships are almost linear. However, for γ_c=0.08%, initial liquefaction was not observed even after a large number of cycles were applied because of the low amplitude of strain applied; hence, the results were not considered.

As Dobry et al. (1985) pointed out, the reciprocals of the slopes of the lines shown in Figure 8 correspond to the volumetric strain. These were read and plotted against the corresponding strain level, as shown in Figure 9. The relationship can be represented by a linear best fit line, as indicated in the figure. The figures are used further on in the analysis to determine the effective stress parameters required in the model.

5.2 Effective stress analysis

In order to investigate the response of Christchurch sites due to the earthquake, an attempt was made to simulate a recorded ground motion at a target liquefied site using one-dimensional (1D) effective stress analysis. For this purpose, the surface acceleration history recorded at Styx Mill Transfer Station, an unliquefied site, was deconvoluted to obtain the motion at the engineering bedrock using the program SHAKE (Schnabel et al. 1972). The computed bedrock motion was then corrected for bearing error (difference between the orientation of the accelerograph at this site and at the target site), and the attenuation law proposed by Campbell (1981) was used to estimate the bedrock motion at the target site.

The target site investigated was the Shirley Library seismic station, where manifestations of liquefaction were observed following the 2011 Christchurch earthquake, but not after the 2010 Darfield earthquake. The site information was obtained from boring logs nearest to the site. In order to investigate the response at this site, effective stress analysis was performed using the computer program DeepSoil (Hashash & Groholski, 2011). In the program, the excess pore water pressure was calculated using the model proposed by Dobry et al. (1985):

$$u_N = \frac{p \cdot f \cdot N_c \cdot F \cdot (\gamma_c - \gamma_t)^s}{1 + f \cdot N_c \cdot F \cdot (\gamma_c - \gamma_t)^s} \tag{12}$$

In the above equation, u_N is the pore pressure generated after N cycles, N_c is the number of cycles, γ_c is the most recent reversal strain, γ_t is the threshold strain, f=1 for 1-D directional generation, and p, s, and F are the effective stress parameters which can be obtained from curve fitting of laboratory test results. These parameters were obtained from the results of the strain-controlled cyclic triaxial tests as follows. Firstly, the parameter p was taken as the value of u^* at large number of cycles, i.e. the inverse of the y-intercept of Figure 8; hence p=1.15. According to Dobry et al. (1985), the parameter F and the threshold strain, γ_t, can be obtained from the slope of the line and x-intercept of Figure 9, i.e. F=4.35 and γ_t=0.02%. Finally, the parameter s was determined through fitting the laboratory test results by the above equation, resulting in s=0.40. Details of the significance of these parameters are discussed by Dobry et al. (1985).

Using effective stress analysis, the ground response of the Shirley Library seismic station site was investigated. The site, represented by the nearest boring data shown in Figure 10(a), consisted of loose sandy deposit with tip resistance between 2-3 MPa up to a depth of about 6.4 m. The water table was assumed to be at GL-1.0 m. In the absence of more information, the engineering

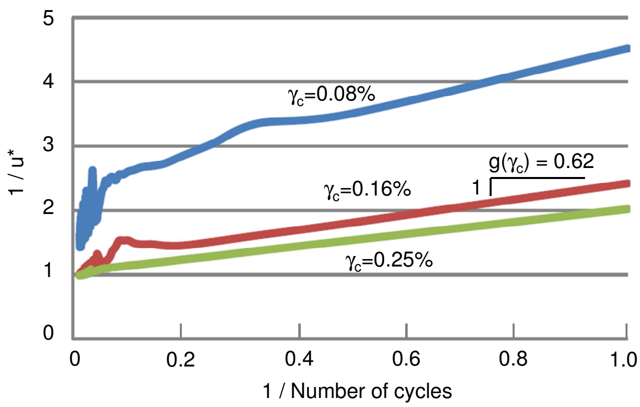

Figure 8 Relationship between excess pore water pressure and number of loading cycles for Christchurch soil.

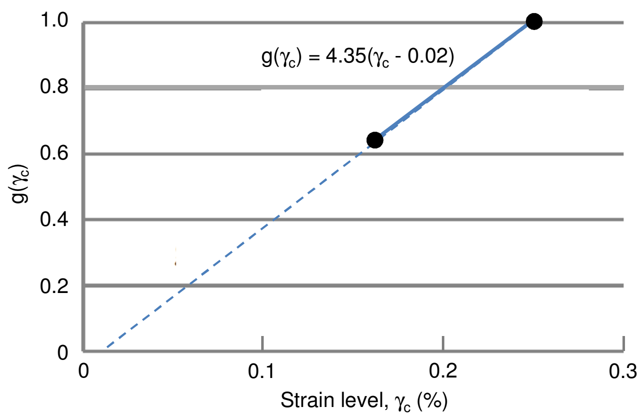

Figure 9 Relationship between volumetric strain and strain level for Christchurch soil.

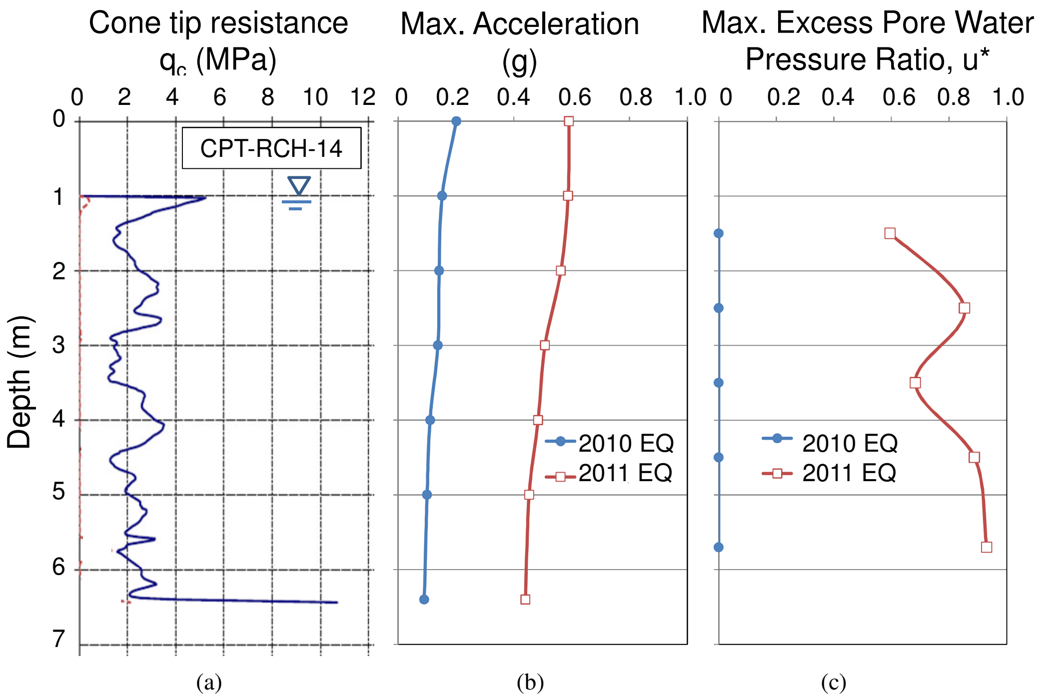

Figure 10 Results of effective stress analysis for Shirley Library Station: (a) CPT penetration profile; (b) distribution of maximum acceleration with depth; and (c) distribution of maximum excess pore water pressure ratio for both 2010 and 2011 earthquakes.

bedrock was assumed at GL-6.4 m. The distributions of the maximum acceleration with depth are shown in Figure 10(b) where it is observed that the input bedrock motion during the 2010 earthquake was only 20% of that during the 2011 earthquake. Considering the thickness of the soft deposit, the amplification of motion for both earthquake events was very small.

Figure 10(c) illustrates the distribution of excess pore water pressure ratio with depth. While excess pore water pressure was not generated during the 2010 earthquake, large pore water pressure ratios, ranging between 0.60-1.0, were observed in the loose saturated sandy deposit at the site during the 2011 earthquake, Obviously, the difference in the amplitude of the bedrock motion between the two events accounted for the generation (or absence) of liquefaction at the site. Note that these observations were consistent with the results of field investigations where manifestations of liquefaction were observed in the vicinity of the strong motion site following the 2011 earthquake, but not after the 2010 earthquake.

Comparisons of the recorded and computed acceleration time histories at the ground surface are shown in Figure 11. For the 2010 earthquake, the computed ground motion is a good match to the recorded one. Since excess pore water pressure was not generated at the site, the analysis was essentially a total stress approach and the effective stress parameters did not play any role. On the other hand, the comparison between the recorded and computed ground surface motions during the 2011 earthquake was quite reasonable, although the period elongation was more prominent in the recorded motion. It is worthy to note that the site considered in the analysis was about 2 km away from the strong motion site and therefore the actual soil profile may be different from what was assumed. As indicated by Brown & Weeber (1992), there is significant variability in soil profiles in Christchurch City.

Finally, a comparison was made between the shear stress-shear strain relations of the deposit at GL-2.5 m for the two events, as shown in Figure 12. The shear stress in the figure has been normalized by the initial effective overburden pressure, σ_{v0}'. The 2010 Darfield earthquake induced very small shear strain at the site, less than the threshold strain for the Christchurch soil; as a result, excess pore water pressure was not generated and the soil essentially behaved elastically. On the other hand, because of the larger cyclic shearing brought about by the larger input acceleration during the 2011 Christchurch earthquake, the deposit was subjected to high

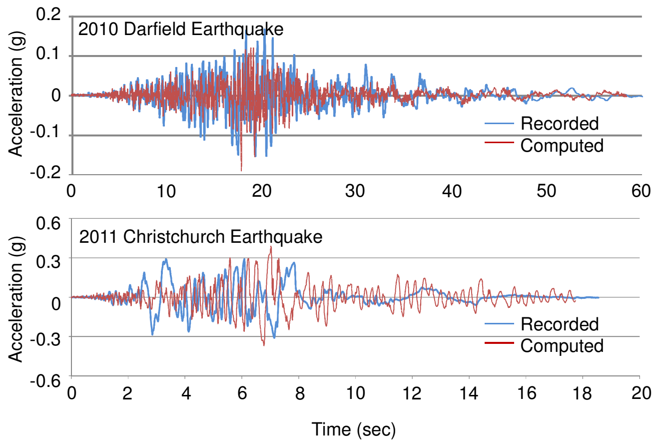

Figure 11 Comparison between recorded and computed ground surface accelerations at Shirley Library seismic station. Top figure: 2010 Darfield earthquake; and bottom figure: 2011 Christchurch earthquake.

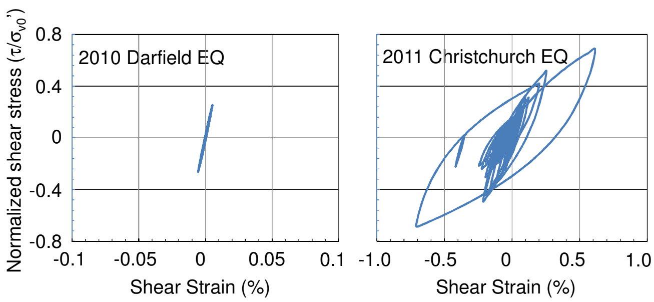

Figure 12 Shear stress – shear strain curves of Shirley Library soil deposit at GL-2.5 m for (a) 2010 Darfield earthquake; and (b) 2011 Christchurch earthquake.

shear strain, as large as 0.7%. As mentioned earlier, excess pore water pressure was generated at this location, inducing larger hysteretic loops with degraded secant modulus.

6. CONCLUDING REMARKS

Christchurch and adjacent areas were battered by large-scale earthquakes over a nine-month period, inducing liquefaction and re-liquefaction over a large region. In this study, maps showing calculated LPIs were produced and comparisons between calculated LPIs and observed damage showed consistent results for eastern Christchurch after both events. Where differences between calculated LPIs and mapped damage were identified, it was found that lateral spreading and the thickness of the non-liquefiable crust layer were the main reasons.

The results of strain-controlled cyclic triaxial tests were used together with readily-available software to simulate the ground motions recorded at the Shirley Library strong motion station following the 2010 and 2011 earthquakes. The effective stress analysis performed was able to explain the occurrence of liquefaction in the February 2011 earthquake and the absence of liquefaction in the September 2010 event.

The scale of damage experienced in Christchurch following the 2011 earthquakes was unprecedented and may be the greatest ever observed in an urban area. The short time interval between these large events has presented a very rare opportunity to investigate re-liquefaction in natural deposits.

7. ACKNOWLEDGMENTS

The authors would like to acknowledge the assistance of Nathan Hickman, Brian Hill, David Bae and Ray Gao, undergraduate students of University of Auckland, in conducting the analyses presented in the paper. The borehole information was provided by Sjoerd van Ballegooy of Tonkin & Taylor.

8. REFERENCES

Beca Carter Hollings & Ferner Ltd (2002) Christchurch Liquefaction - Study Stage II ECAN Report. Christchurch, New Zealand.

Brown, L. J. & Weeber, J. H. (1992) Geology of the Christchurch Urban Area. Scale 1:25000, Lower Hutt, Institute of Geological & Nuclear Sciences Limited.

Campbell, K.W. (1981) "Near-source attenuation of peak horizontal acceleration". Bulletin of the Seismological Society of America, 71: 2039-2070.

Cubrinovski, M. & Taylor, M. (2011) Liquefaction Map - Drive-through Reconnaissance, NZSEE Website http://www.nzsee.org.nz/

Dobry, R., Pierce, W.G., Dyvik, R., Thomas, G.E. and Ladd, R.S. (1985) Pore pressure model for cyclic straining of sand. Research Report, Dept. of Civil Engineering, Rensselaer Polytechnic Institute, Troy, N.Y., 56pp.

GeoNet (2011) Strong motion FTP site, ftp://ftp.geonet.org.nz/strong/processed/Proc/2011/02_Christchurch_mainshock_extended_pass_band/

Gledhill, K., Fry, B., Ristau, J., Holden, C. & Reyners, M. (2011) "The Darfield (Canterbury, New Zealand) Mw 7.1 Earthquake of September 2010: A Preliminary Seismological Report". Seismological Research Letters, Vol. 82, No. 6, 378-376.

Hashash, Y.M.A & Groholski, D.R. D. (2011) DEEPSOIL V4.0, User Manual and Tutorial, 98 p.

Ishihara, K. (1985) "Stability of natural deposits during earthquakes". 11th International Conference on Soil Mechanics and Foundation Engineering.

Iwasaki, T., Arakawa, T. & Tokida, K. I. (1984) "Simplified procedures for assessing soil liquefaction during earthquakes". International Journal of Soil Dynamics and Earthquake Engineering, 3, 49-58.

Kiyota, T., Hosono, Y. and Yamada, S. (2011) "Results of field survey on the latest earthquake on 13th June, 2011, in Christchurch city". Unpublished Report, 5pp.

Natural Hazards Research Platform, NHRP (2011) "Why the 2011 Christchurch earthquake is considered an aftershock". http://www.naturalhazards.org.nz.

Orense, R.P., Kiyota, T., Yamada, S., Cubrinovski, M., Hosono, Y., Okamura, M., Yasuda, S. (2011) "Comparative study of liquefaction features observed during the 2010 and 2011 Canterbury earthquakes". Seismological Research Letters, Vol. 82, No. 6, 905-918.

Robinson, K., Cubrinovski, M., Kailey, P. & Orense, R. P. (2011) "Field Measurements of Lateral Spreading following the 2010 Darfield Earthquake". Ninth Pacific Conference on Earthquake Engineering. Auckland, New Zealand

Robertson, P. K. & Cabal, K. L. (2010) Guide to Cone Penetration Testing for Geotechnical Engineering, Gregg Drilling & Testing, 4th Edition.

Robertson, P. K. & Wride, C. E. (1998). "Evaluating cyclic liquefaction potential using the cone penetration test". Canadian Geotechnical Journal, 35, 442-459.

Schnabel, P., Lysmer, J. & Seed, H. B. (1972) "SHAKE: Equivalent Linear Seismic Response Analysis of Horizontally Layered Soil Deposits". Report No. EERC 72-12. Earthquake Engineering Research Center, University of California, Berkeley. CA

Seed, H. B. & Idriss, I. M. (1970) "A Simplified Procedure For Evaluating Soil Liquefaction Potential". Earthquake Engineering Research Centre. Berkeley, California, College of Engineering, University of California

Tonkin & Taylor Co. Ltd. (2010) Darfield Earthquake 4 September 2010 Geotechnical Land Damage Assessment & Reinstatement Report - Stage 1 Report.

Youd, T. L., Idriss, I. M., Andrus, R. D., Arango, I., Castro, G., Christian, J. T., Dobry, R., Liam Finn, W. D., Harder L.F, Jr., Hynes, M. E., Ishihara, K., Koester, J. P., Liao, S. S. C., Marcuson III, W. F., Martin, G. R., Mitchell, J. K., Moriwaki, Y., Power, M. S., Robertson, P. K., Seed, R. B. & Stokoe II, K. H. (2001) "Liquefaction resistance of soils: Summary report from the 1996 NCEER and 1998 NCEER/NSF workshops on evaluation of liquefaction resistance of soils". Journal of Geotechnical and Geoenvironmental Engineering, 127, 817-833